Proceedings - 19th International Conference - IEEE/EMBS Oct. 30 - Nov. 2, 1997 Chicago, IL. USA

COMPUTED TOMOGRAPHY IMAGE RESTORATION USING CONVEX-POTENTIAL 3-D MARKOV RANDOM FIELDS

Nicolas Villain and Yves Goussard

École Polytechnique
Biomedical Engineering Institute
C.P. 6079, Station Centre-Ville
Montréal (Québec)
H3C 3A7, Canada
villain@grbb.polymtl.ca

Stéphane Brette and Jérôme Idier

Laboratoire des Signaux et Systèmes
École Supérieure d'Électricité
Plateau de Moulon
91192 Gif-sur-Yvette Cedex
France
idier@lss.supelec.fr

ABSTRACT

In order to design and manufacture custom-fitted prostheses of the knee joint, one must perform a very accurate geometric reconstruction of the bone surface from computed tomography images. This communication deals with the image restoration used to improve the reconstructed images. In the Bayesian context of *maximum a posteriori* estimation, edge-preserving Markov random fields as an *a priori* model for the images have proven to give very good results. To avoid dealing with nonconvex optimization, we adopt the elegant method proposed in [1]. This approach leads to a very efficient single site update algorithm and an analytical formulation can be found for convex edge-preserving potentials. Moreover, we propose to define a three dimensional Markov random field to take into account the geometry of computed tomography. The resulting restoration allows good recovery of the sharp discontinuities between the bone and soft tissues and the accuracy is significantly improved by the three dimensional model.

1. INTRODUCTION

Our work is part of a joint project whose aim is to design and manufacture custom-fitted prostheses of the knee joint from a series of computed tomography (CT) images. In order to ensure a sufficient lifespan for the prothesis which undergoes important strain, the congruence between its surface and the bone itself should be less than 1 mm. Hence the need for a very accurate extraction of bone surface geometry.

Partial support for this work was provided by the Natural Science and Engineering Research Council of Canada under Research Grant # OGP013 8417.

To improve this extraction, we can introduce image restoration as a first step before surface reconstruction. In addition to blur and noise reduction, the sharp discontinuities separating the fairly homogeneous areas of bone and soft tissues have to be restored accurately. In this communication we present a three dimensional (3-D) approach designed to meet these somewhat contradictory requirements.

The problem of image restoration is known to be ill-posed — the mathematical formulation involves ill-conditioned matrices. Regularization methods can be seen as the addition of *a priori* constraints to solve this problem. Here, we adopt a Bayesian approach in which the *a priori* information is specified under the form of probability density functions (PDFs) of the original object to be restored and of the noise. A simple noise model is often satisfactory, while finding a well adapted *a priori* model of the object is more complicated. To model homogeneous regions separated by sharp discontinuities, Markov-Gibbs random fields (MRFs) have often been chosen [2] because they are based upon local pixel interactions. Moreover, Gibbs potentials used in MRFs can be customized to achieve sharper restoration than with the classical quadratic (i.e., Gaussian) *a priori* models. But, the MRFs designed to restore sharp discontinuities often yield nonconvex criteria [3], and require complex optimization techniques.

However, the use of particular MRFs yielding convex criteria associated with the application of convex analysis results allows us to design efficient restoration methods [1]. In this communication, we propose to apply these principles to edge-preserving restoration of CT images. Moreover, since tomographic images are 2-D slices of a 3-D object, the 3-D information should be taken into account. We thus define a 3-D MRF which is a natural extension of 2-D MRFs [4], use it as

(0-7803-4262-3/97/$10.00 (C) 1997 IEEE)

the *a priori* model of the object under investigation and develop the corresponding 3-D restoration method.

2. APPROACH

The original 3-D object $\boldsymbol{x}$ is observed through a CT scanner which is considered a linear system with a two dimensional point spread function (PSF) H. Although perfect scanners should have a 2-D PSF, partial volume effects and X-ray diffusion from neighboring slices make this assumption an approximation. Moreover, the PSF is assumed to be spatially invariant because we have found that its variations induced negligible effects on restoration. Thus, the image formation model with additive noise can be expressed in matrix form:

$$\boldsymbol{y} = \boldsymbol{H}\boldsymbol{x} + \boldsymbol{n} \tag{1}$$

where $\boldsymbol{H}$ is the convolutional matrix constructed from the PSF H.

In the Bayesian framework introduced in the previous section, we need to define the PDF of the original object to be restored as well as the PDF of the noise. The *a priori* model $p(\boldsymbol{x})$ and the noise model $p(\boldsymbol{n})$ represent the *a priori* information we introduce to solve the ill-posed inverse problem of restoration. We then select the *maximum a posteriori* (MAP) estimator because it yields a very effective and adaptable criterion.

With standard application of Bayes rule, the MAP estimate $\widehat{\boldsymbol{x}}$ can be expressed as a function of the *a priori* model and of the likelihood $p(\boldsymbol{y}|\boldsymbol{x})$ derived from the noise model:

$$\widehat{\boldsymbol{x}} = \arg\max_{\boldsymbol{x}}[p(\boldsymbol{x}|\boldsymbol{y})] \propto \arg\max_{\boldsymbol{x}}[p(\boldsymbol{x})p(\boldsymbol{y}|\boldsymbol{x})] \tag{2}$$

The noise is simply modeled as white Gaussian noise with known variance σ_n^2. Given (1), the expression of $p(\boldsymbol{y}|\boldsymbol{x})$ is derived from the Gaussian PDF of the noise:

$$p(\boldsymbol{y}|\boldsymbol{x}) = K \exp\left\{-\frac{\|\boldsymbol{y} - \boldsymbol{H}\boldsymbol{x}\|^2}{2\sigma_n^2}\right\} \tag{3}$$

The choice of an *a priori* PDF of the object to be restored is more delicate. To represent the structure of the original object, equivalence between Markov and Gibbs random fields yields an expression of the *a priori* PDF with Gibbs potentials V_c defined on each set c (called clique) of neighboring voxels:

$$p(\boldsymbol{x}) = \frac{1}{Z} \exp\left\{-\lambda \sum_{c \in \mathcal{C}} V_c(\boldsymbol{x})\right\} \tag{4}$$

It is more convenient to substitute (4) and (3) in the neglog equivalent of (2) i.e. $\widehat{\boldsymbol{x}} = \arg\min_{\boldsymbol{x}}[J(\boldsymbol{x})]$

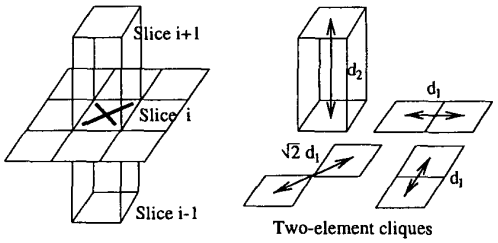

Figure 1: Chosen 3-D neighborhood of a given voxel and corresponding two-element cliques

with:

$$J(\boldsymbol{x}) = \frac{\|\boldsymbol{y} - \boldsymbol{H}\boldsymbol{x}\|^2}{2\sigma_n^2} + \lambda \sum_{c \in \mathcal{C}} V_c(\boldsymbol{x}) \tag{5}$$

where the set of cliques $\mathcal{C}$ and the potentials V_c are still to be defined. In the next section, we will give a detailed description of these parameters of the *a priori* MRF.

3. CHOICE OF MRF

First, we need to define a neighborhood system with the corresponding set of cliques $\mathcal{C}$. Then, we will describe the Gibbs potentials defined on the cliques.

As $\boldsymbol{x}$ is modeled as a 3-D, the neighborhood includes voxels from the same and the nearest slices. Since the cross-slice distance is greater than cross-voxel distances within the same slice, our choice of neighborhood of a given voxel includes the 8 nearest voxels from the same slice and the nearest voxels of the upper and lower slices as shown in Fig. 1.

We then define Gibbs potentials only on $\mathcal{C}_2$, the set of two-voxel cliques, as cost functions ϕ of the gradient u_c inside the cliques.

$$u_c = \frac{x_r - x_s}{d(r,s)} \tag{6}$$

where $d(r,s)$ is the distance between voxels r and s. With such cliques (shown in Fig. 1), $d(r,s)$ can only take three different values: d_1 for two nearest voxels of the same slice, $\sqrt{2}d_1$ for a diagonal clique in the same slice and $d_2 > d_1$ for a clique between two different slices. The criterion becomes:

$$J(\boldsymbol{x}) = \frac{\|\boldsymbol{y} - \boldsymbol{H}\boldsymbol{x}\|^2}{2\sigma_n^2} + \lambda \sum_{c \in \mathcal{C}_2} \phi(u_c) \tag{7}$$

The choice of the cost functions $\phi(u)$ is not only guided by the accuracy of the *a priori* model but also

by implementation and practical considerations. Nonconvex potential MRF are more likely to be edge-preserving and lead to better representation of real objects. But they yield a nonconvex criterion and we have already mentioned the complexity related to nonconvex optimization: gradient descent algorithms can get trapped in local minima and more elaborate algorithms are numerically demanding. To avoid these difficulties, convex potentials with better edge-preserving capabilities than simple quadratic forms have been proposed [5]. A good compromise is reached when $\phi(u)$ is quadratic for small values of u and linear for large values. The function we propose exhibits such behavior. It takes the following form:

$$\phi(u) = \sqrt{1 + (\frac{u}{\delta})^2} \tag{8}$$

where δ is a scaling factor determining the transition between the quadratic and linear regions.

4. OPTIMIZATION

Now that the *a priori* model is precisely known, image restoration consists of the minimization of the criterion defined in (7). Our choice of convex potentials yields a convex criterion so that simple optimization algorithms can be used.

The whole set of observations $\boldsymbol{y}$ are needed to restore the 3-D object $\boldsymbol{x}$. With M slices of $N \times N$ pixels, $\boldsymbol{x}$ is composed of $M \times N \times N$ voxels. Even with a convex criterion, the optimization can be numerically burdensome. For instance, global update algorithms, such as gradient descent methods, require the evaluation of the criterion and its gradient at least once per iteration. On the contrary, single site update algorithms, like Gauss-Siedel (GS) or successive over-relaxation (SOR), handle only local subsets of the object. GS optimization consists of successively minimization with respect to individual voxels. Convergence toward the global minimum is guaranteed by the convexity of the criterion. Each voxel update can be written as:

$$x_i \leftarrow x_i^{new} = m_i = \arg\min_{x_i} J(\boldsymbol{x}) \tag{9}$$

But, to allow faster convergence, we use the SOR algorithm, where the correction of each voxel is multiplied by a factor α such that $1 < \alpha < 2$:

$$x_i \leftarrow x_i^{new} = x_i + \alpha(m_i - x_i) \tag{10}$$

Now, the problem is to evaluate m_i for each voxel. With nonquadratic potentials, such as the one we defined in (8), m_i can not be expressed in closed-form. Once again, given the number of voxels, computing m_i iteratively can become impractical. However, for almost any convex potential, the introduction of auxiliary variables $\boldsymbol{l}$ [1, 6] allows us to define an extended criterion $J(\boldsymbol{x}, \boldsymbol{l})$ which is quadratic with respect to x_i:

$$J(\boldsymbol{x}, \boldsymbol{l}) = \frac{\|\boldsymbol{y} - \boldsymbol{H}\boldsymbol{x}\|^2}{2\sigma_n^2} + \lambda \sum_{c \in \mathcal{C}_2} \left[l_c (u_c)^2 + \psi(l_c) \right] \tag{11}$$

where ψ is defined so that $J(\boldsymbol{x}) = \min_l J(\boldsymbol{x}, \boldsymbol{l})$ which is equivalent to:

$$\phi(u) = \min_l \left[l(u)^2 + \psi(l) \right] \tag{12}$$

By definition, (12) means that $\phi(\sqrt{|u|})$ has to be the concave conjugate of $-\psi(l)$. It is possible because, with the form proposed in (8), $\phi(\sqrt{|u|})$ is concave. In this case, according to a duality principle [7], if $-\psi(l)$ is defined as the concave conjugate of the concave function $\phi(\sqrt{|u|})$ (i.e. if $-\psi(l) = \min_u [lu - \phi(\sqrt{|u|})]$), then, in turn, $\phi(\sqrt{|u|})$ is also the concave conjugate of $-\psi(l)$ and (12) holds. The two functions are said to be concave conjugates.

Using the previous construction, the extended criterion J($\boldsymbol{x}$,$\boldsymbol{l}$) shares the same minimum as $J(\boldsymbol{x})$ and is also convex. Thus, the minimization of $J(\boldsymbol{x}, \boldsymbol{l})$ can be performed alternatively with respect to the voxels x_i and to the auxiliary variables l_c. For the voxels, the extended criterion is quadratic with respect to x_i and an analytic expression of m_i can be used. For the auxiliary variables, the definition of ψ also yields an analytic solution: $l_c \leftarrow l_c^{new} = \phi'(u_c)/2u_c$. The algorithm scans the whole volume and iterates the process until a stopping rule is fulfilled [1].

5. RESULTS

In order to evaluate the accuracy of the 3-D restoration method, we used a CT scanner with a known PSF and a phantom of known dimensions — an ellipsoid immersed in water. A CT scan of the phantom was performed and our algorithm was applied on the resulting CT images. Finally, the restored images were compared to the phantom. Fig. 2 gives the example of a particular slice: the restored image shows satisfactory noise reduction and the edges are sharper.

But, as mentioned earlier, our work is only the first step in the whole surface reconstruction process. Eventually, the restoration has to be judged by the accuracy of the final surface. Since exact measurements of the congruence between reconstructed and original surfaces are not available yet, we applied a contour extraction algorithm to the restored images. The results were compared to those obtained with the corresponding 2-D MRF. As expected, Fig. 3 shows significant

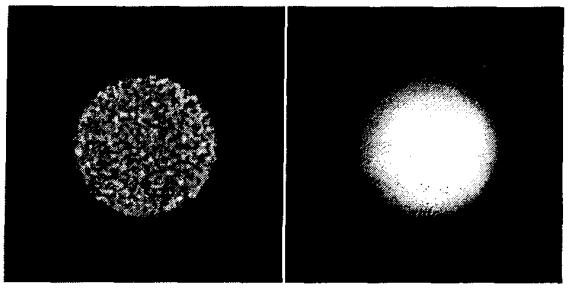

Figure 2: Raw 320 × 320 CT image and restored image of a slice of the phantom (an ellipsoid of known dimensions).

improvement when using the 3-D model because the 3-D nature of the

improvement - Command not found object is taken into account. With 3-D data, the noise has a reduced influence and restored contours are more regular. What is more, the improvement is worth the higher computational cost related to the 3-D MRF because only the 3-D model reaches the accuracy required in our context.

6. CONCLUSION

To restore CT images, we have developed a method based on a 3-D MRF as an *a priori* model of the original object. The use of edge-preserving convex potentials yields a convex criterion with an interesting compromise between accurate restoration and implementation complexity. With slightly higher computational cost than the corresponding 2-D method, this 3-D restoration method provides increased accuracy because all the CT images are treated together to take into account the 3-D information. But the optimization is done locally and the convergence is guaranteed by the convexity of the criterion.

7. REFERENCES

[1] S. Brette and J. Idier, "Optimized single site update algorithms for image deblurring," in *Proc. Intl. Conf. Image Proc.*, Lausanne, Switzerland, 1996.

[2] C. Bouman and K. Sauer, "A generalized Gaussian image model for edge-preserving MAP estimation," *IEEE Trans. Image Processing*, vol. 2, no. 3, pp. 296–310, July 1993.

[3] A. Blake and A. Zisserman, *Visual Reconstruction*, MIT Press, Cambridgem MA, 1987.

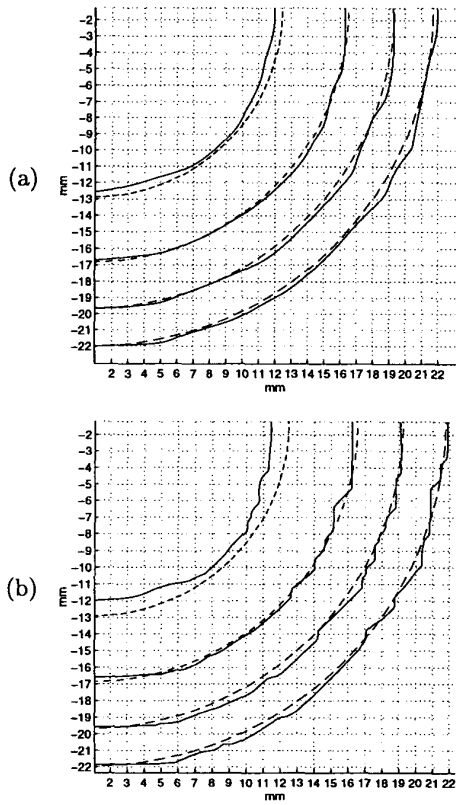

Figure 3: Contours from a sequence of slices of the phantom obtained (a) with our 3-D model compared to the original contours (dashed line) and (b) with a similar model with a 2-D MRF compared to the original contours (dashed line)

[4] H. Derin and P. A. Kelly, "Discrete-index Markov-type random processes," *Proc. IEEE*, vol. 77, pp. 1485–1510, 1989.

[5] P. J. Green, "Bayesian reconstructions from emission tomography data using a modified EM algorithm," *IEEE Trans. Medical Imaging*, vol. 9, pp. 84–93, March 1990.

[6] Stuart Geman and Georges Reynolds, "Constrained restoration and recovery of discontinuities," *IEEE Trans. Pattern Anal. Mach. Intell.*, vol. PAMI-14, no. 3, pp. 367–383, March 1992.

[7] D.G. Luenberger, *Optimization by Vector Space Methods*, Wiley, New York, NY, 1 edition, 1969.